ChemComm

Accepted Manuscript

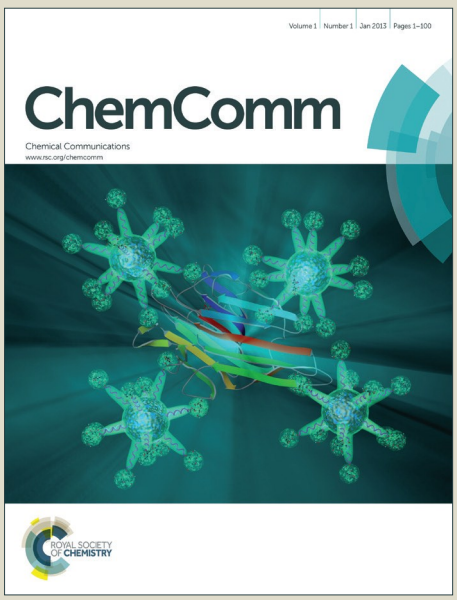

ROYAL SOCIETY OF CHEMISTRY

www.rsc.org/chemcomm

Chemical Communications

COMMUNICATION

Manipulation and Measurement of pH sensitive Ligand-Metal Binding Using Electrochemical Proton Generation and Metal Detection

Received 00th January 20xx,
Accepted 00th January 20xx

DOI: 10.1039/x0xx00000x

www.rsc.org/

Tania L. Read,[a] Maxim B. Joseph[a] and Julie V. Macpherson[a*]

Generator-detector electrodes can be used to both perturb and monitor pH dependant metal-ligand binding equilibria, *in-situ*. In particular, protons generated at the generator locally influence the speciation of metal (Cu^{2+}) in the presence of ligand (triethylenetetraamine), with the detector employed to monitor, in real time, free metal (Cu^{2+}) concentrations.

Many important chemical processes, such as acid-base; hydrolysis; complexation; extraction, redox; solubility and precipitation, are governed by a pH dependent chemical equilibrium.[1] Experimentally, analysis of the change in species concentration (or activity) with pH is often carried out using different solutions of varying (and known) pH. However, for certain reactions it is advantageous not only to be able to investigate the process *in-situ* but also to locally manipulate solution pH; pushing the pH dependent equilibrium in a preferred direction.

pH dependent metal-ligand complexation is of importance in a wide range of fields, including medicine[2] e.g. chelation treatments for cancer therapy,[3] waste water treatment,[4] environmental research e.g. toxic metal availability in aqueous solutions and human function,[5] for example the binding of oxygen to haemoglobin in blood.[6] To illustrate the concept of pH manipulation and show how by careful control of local solution pH we can control the extent of metal-ligand binding, *in-situ*, we focus on aqueous heavy metals, a key concern due to their toxicity.[7] For many cases, the free (labile) species is bioavailable and therefore more toxic than the complexed species and is often of primary interest.[8] However, as the bound species acts as a reservoir of free species that can be released when the equilibrium shifts, due to e.g. a pH change,[9] understanding the pH dependent relationship and manipulating it during measurement can be important.

Concentrations of free and complexed metal species are often measured using techniques such as UV-Vis spectroscopy[10], inductively coupled plasma mass spectrometry (ICP-MS) or optical emission spectrometry,[11] voltammetry[12] and potentiometry, [13] thermometry[14] and conductometry.[15] The majority of these techniques do not provide information on the individual concentrations of both the free species and the ligand bound metal species. For example, ICP-MS will measure total metal concentration, whilst voltammetry and related techniques, measure only the free metal ion concentration (at the given measurement pH).[16]

Electrochemistry is a popular method for detection of aqueous species,[7] due to its relative ease of use and low cost, and its potential for application *in situ*; removing the necessity to take samples away from the real environment for analysis, which can affect the equilibrium of the sample and give false measurements of free *vs.* bound species.[17] Interest in pH control via electrochemical methods is evident,[18],[19] with applications such as pH titration,[20] chemical species quantification[21] *etc* already highlighted.

For this study we focus on copper,[22] a heavy metal identified as being of key concern worldwide due to both its prevalence as a trace metal and its toxicity.[23] Although necessary in small quantities in the body copper is also extremely toxic when absorbed in excess, causing oxidative stress damage to organs; copper has also been linked to Alzheimer's disease.[24] For pH dependent ligand binding studies, triethylenetetramine (TETA), serves as a model system for Cu^{2+} complexation. TETA is a therapeutic molecule used in the treatment of Wilson's disease, the latter characterized by copper accumulation in vital organs of the body.[25]

$$Cu^{2+}(aq) + TETA \leftrightarrows Cu[TETA]^{2+} \qquad [1]$$

TETA has four protonation constants, log K_p, (log K_1 = 9.79, log K_2 = 9.11, log K_3 = 6.68, and log K_4 = 3.28).[26] The un-protonated (TETA) and singly protonated (HTETA) can bind to Cu^{2+}, whilst the two, three and four pronated (H_2,H_3,H_4) TETA ligands cannot. The pH dependent speciation curves for the Cu^{2+} TETA system can be determined using MINEQL+ chemical equilibrium modelling software in conjunction with known values for β[26] the complex formation constant and K_p, where:

$$\log \beta = \sum \log K_p \qquad [2]$$

Figure 1(a) shows the speciation curves, expressed as % of total copper concentration, for free Cu^{2+} (black line), $Cu[HTETA]^{3+}$ (blue line), $Cu[TETA]^{2+}$ (red line) and combined $Cu[TETA]^{2+}$ + $Cu[HTETA]^{3+}$ (purple line) as a function of pH

[a] Department of Chemistry, University of Warwick, Gibbet Hill Road, Coventry, CV4 7AL.

over the range 1 – 10, for 100 μM Cu^{2+} and 100 μM TETA. At pH values < 2.5, all Cu^{2+} exists in the free form, whilst for pH values ≥4.46, all the Cu^{2+} is bound to TETA ligands and therefore not freely available.

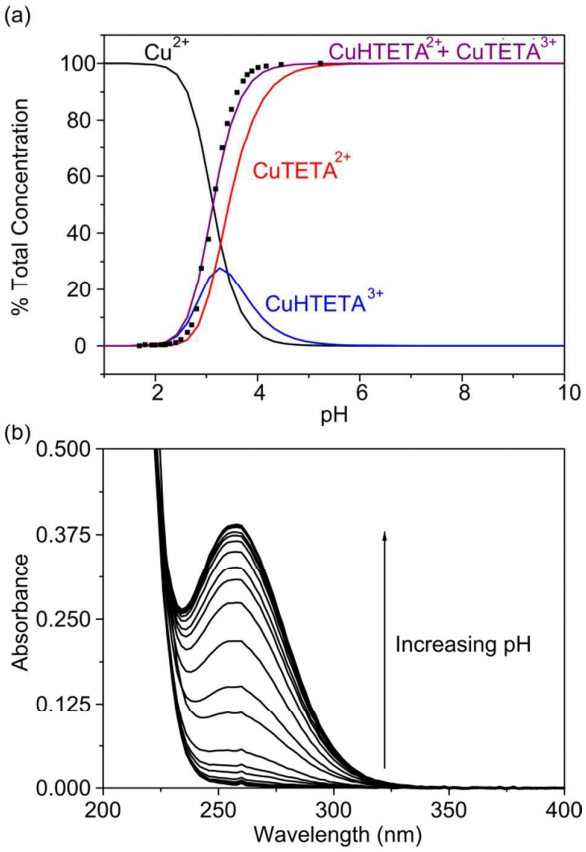

Figure 1. (a) Simulated speciation curves for 100 μM Cu^{2+} ($Cu(NO_3)_2$) and 100 μM TETA (ionic strength = 300 μM) across the pH range 1 - 10, expressed as % of total copper for free Cu^{2+} (black), $Cu[HTETA]^{3+}$ (blue), $Cu[TETA]^{2+}$ (red) and total $Cu[HTETA]^{3+}$ + $Cu[TETA]^{2+}$ (purple). (b) UV-Vis data, corresponding to $Cu[HTETA]^{3+}$ + $Cu[TETA]^{2+}$ for a pH titration of 100 μM Cu^{2+} and 100 μM TETA mixture via 25 dropwise additions of HCl (starting pH = 5.23, end pH = 1.69). Peak maxima / peak maximum (for maximum absorbance) × 100 % (■) is plotted on (a).

To verify the modelled speciation data, UV-Vis (Varian, Cary 50 Bio UV-Visible Spectrometer) titration data was obtained by dropwise addition of 0.1 M HCl to a mixture of 100 μM Cu^{2+} and 100 μM TETA in a stirred solution. Between additions the pH value was measured using a pH probe (Mettler Toledo) and a ~3 cm^3 sample taken for UV-Vis absorbance measurements in a quartz cuvette (1 cm^2 cross-section, optical path length 1 cm). The resulting absorbance data, over 200 nm - 400 nm, for pH's in the range 1.69 – 5.23, is shown in **Figure 1(b)**. An absorption maxima is observed at ~250 nm which is in good agreement with that seen previously for the $Cu[TETA]^{2+}$ ligand-metal complex (absorptivity ~ 3900 M^{-1} cm^{-1}).[26] The absorption characteristics for $Cu[HTETA]^{3+}$ are expected to be very similar to those for $Cu[TETA]^{2+}$ and therefore the peak maximum is likely to represent the absorption characteristics of both species (*vide infra*). Note free (hydrated) Cu^{2+} should be visible in the range 500 - 900 nm,[27] however given its low absorption coefficient,[27] in combination with the concentrations employed here, a measurable signal was not discernible. The absorption data is presented as (peak maximum for a given pH value) / (peak maximum for 100 % bound Cu^{2+} *i.e.* for pH values ≥ 4.46) × 100 % (■) and displayed on **Figure 1(a)**. As shown there is a good fit between the experimental UV-Vis data achieved and the simulated speciation curve for combined $Cu[TETA]^{2+}$ and $Cu[HTETA]^{3+}$, confirming that the experimental UV-Vis peak maximum most likely represents the absorption of both $Cu[TETA]^{2+}$ and $Cu[HTETA]^{3+}$.

In order to be able to generate local pH changes *in-situ* the use of a dual electrode system is proposed. We use conducting boron doped diamond (BDD) as it has recently been shown that BDD is ideally suited to galvanostatic generation of proton or hydroxide fluxes.[19] Moreover, a BDD electrode is stable (does not degrade or show surface instabilities due to erosion or oxidation/reduction of the surface) under the required high applied current densities, for long periods of time, in contrast to thin film metal electrodes.[28] The concept employed herein is illustrated schematically in **Figure 2** and uses the outer (ring) electrode to controllably generate a quantitative flux of protons by the oxidation of water in the presence of $Cu[TETA]^{2+}$ to systematically change the position of equilibrium from fully bound Cu^{2+} to free Cu^{2+}. The central detector (disc) electrode, works on voltammetric principles and thus only detects free Cu^{2+}, by electrochemical reduction to metallic Cu, and subsequent electrochemical dissolution (stripping) from the electrode surface (anodic stripping voltammetry; ASV).[7, 29]

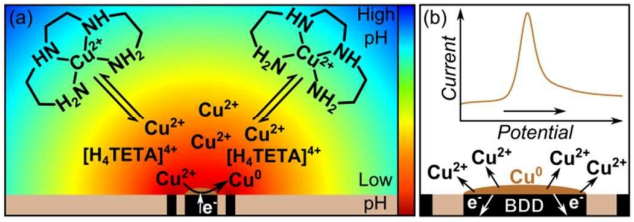

Figure 2. Schematics showing (a) generation profile of protons at the ring electrode of the ring-disc, dual electrode system. The increase in solution pH in the vicinity of the disc perturbs the Cu^{2+} - TETA equilibrium, releasing free Cu^{2+} into solution for subsequent reduction at the disc electrode. (b) The electrodeposited Cu is subsequently detected on the disc electrode via re-oxidation (dissolution) using anodic stripping voltammetry.

Fabrication of the BDD dual (ring-disc) electrode is described in further detail in Electronic Supporting Information Section 1, but briefly involved laser machining a 500 μm radius cylinder and a 50 μm width hollow cylinder (outer radius = 810 μm and inner radius = 760 μm) from a 600 μm thick wafer of freestanding *i.e.* not attached to a growth substrate, high quality (minimal sp^2 content) conducting BDD.[19a] The electrodes were assembled in insulating epoxy and the top surface polished flat, using silicon carbide, to ensure a co-planar arrangement of electrodes and insulator. The separation between the ring and disc was ~260 μm.

The electrochemical set-up is described in detail in ESI, Section 2. Initial "bulk pH" experiments used the BDD detector (disc) electrode to detect Cu^{2+} using ASV, in solutions containing 100 μM Cu^{2+} and 100 μM TETA with 0.1 M KNO_3 added as a supporting electrolyte, to suppress migration effects. In these experiments, the pH of the solution was changed by deliberately adding either HNO_3 or KOH to produce solutions

with pH values in the range 2.50 – 5.01 For each solution, the electrode was held at -0.5 V versus SCE, for 60 s, sufficient to provide a large enough overpotential for copper electrodeposition, but not negative enough to reduce protons in solution. Note, electro-generated oxygen reduction, for the pH range investigated, was found to be minimal, at this potential, on Cu electrodeposited BDD. ASV experiments were performed immediately following electrodeposition by scanning in a positive potential direction using linear sweep voltammetry from -0.25 V to +0.5 V at a potential scan rate of 0.1 V s^{-1}.

Figure 3(a) shows the ASV current-voltage signals for stripping voltammetry experiments in 100 µM Cu^{2+} and 100 µM TETA solutions adjusted to bulk pH values of 2.5, 2.99, 3.52, 4.05, and 5.01. At pH 5.01, no electrochemical signal is seen, as expected based on the fact that Cu^{2+} is fully complexed with TETA and electrochemically inaccessible. As the pH is decreased and TETA becomes protonated, forming first HTETA then increasing in protonation, until fully protonated (H_4TETA), Cu^{2+} ions are released from the metal-ligand complex and are freely available for electroreduction. The lower the pH the more Cu^{2+} available for electroreduction (until it has all been released), this manifests itself in an increasing peak height (and area under the curve) as the pH of the solution is lowered.

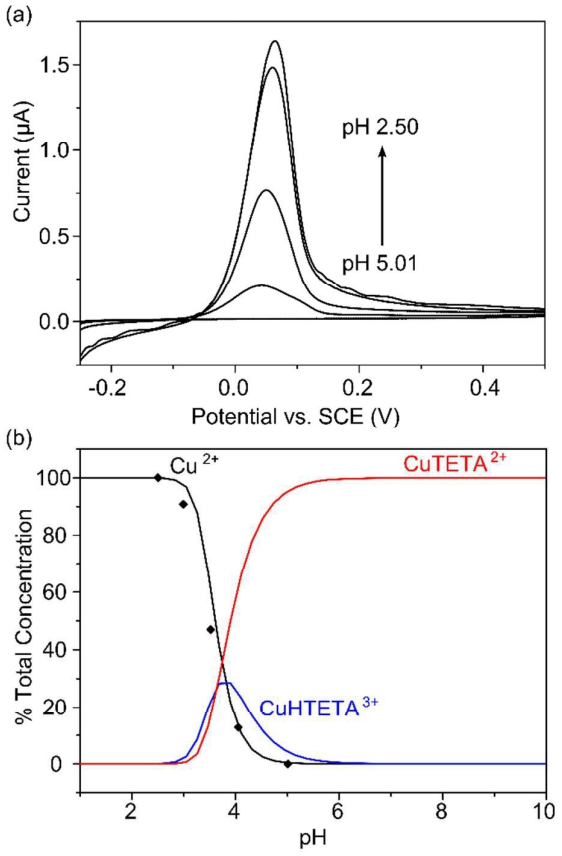

Figure 3. (a) ASV curves for Cu^{2+} stripping for solution pH values in the range 2.50, 2.99. 3.52, 4.05, 5.01, in a 100 µM Cu^{2+} and 100 µM TETA solution with 0.1 M KNO_3 added as supporting electrolyte, scan rate = 0.1 V s^{-1}. (b) ASV (i_p / $i_{p,max}$ × 100 %) data (♦) plotted as a function of pH. Also shown are the simulated speciation curves for the equivalent solution experimental conditions for free Cu^{2+} (black), $Cu[HTETA]^{3+}$ (blue), $Cu[TETA]^{2+}$ (red), ionic strength = 0.1003 M.

The simulated Cu^{2+} TETA speciation curve is shown in **Figure 3(b)**, adjusted to account for the change in ionic strength of the solution due to the presence of supporting electrolyte (KNO_3) in the electrochemical experiment. Note NO_3^- shows a characteristic absorption at ~210 - 220 nm[30] in the UV-Vis spectra and therefore cannot be added to the solutions in **Figure 1(a)**. The peak current, i_p, (♦) normalized with respect to the maximum, $i_{p,max}$ recorded under acidic conditions, where the Cu^{2+} is completely unbound, × 100 %, is shown also on **Figure 3(b).** It is clear that for the ASV experiments recorded in the different pH solutions there is good agreement between the electrochemical signal which relates to free Cu^{2+} and the speciation curve for free Cu^{2+}, under these solution conditions.

Experiments were then carried out under bulk pH = 6.4 conditions. A constant current (in the range 0.10 – 2 mA cm^{-2}) was applied to the generator electrode (versus a Pt counter electrode) for a period of 300 s to generate a steady-state flux of protons (via oxidation of water); the higher the current density the greater the flux. Note higher than 6 mA cm^{-2} causes significant bubbles (oxygen) to form which can be problematic for copper electrodeposition and stripping. With the current still applied, the potential at the detector electrode was then switched on (-0.5 V for 60s, versus SCE) to electrodeposit any free Cu^{2+} onto the electrode surface and then swept anodically between -0.25 V and +0.5 V at 0.1 V s^{-1} to remove electrodeposited Cu from the surface. The resulting (i_p / $i_{p,max}$ × 100 %) data, derived from the recorded ASV's (normalised and shown in ESI, section 3) during *in-situ* pH generation is displayed in **Table 1**.

Importantly, the same trend can be observed in **Table 1** as for **Figure 3(a),** where increasing the applied current density, which causes a decrease in the local solution pH, causes the ASV stripping peak currents to increase in size. The maximum peak current was recorded for a galvanostatic current of 1.98 mA cm^{-1}. Applied current densities greater than this gave similar peak currents. Currents of ≥ 1.98 mA cm^{-2} were therefore assumed to have made the local solution sufficiently acidic to free the Cu^{2+} and fully protonate the TETA. Using the speciation curve in **Figure 3(b)** and by plotting the observed (i_p / $i_{p,max}$ × 100%) it was possible to estimate the local pH at the electrode surface for the different applied galvanostatic currents, also shown in **Table 1**.

In summary, we have shown that using an electrochemical proton generator coupled to an electrochemical measurement (detector) system it is possible to both change and monitor the speciation of a pH sensitive metal-ligand complex, *in-situ*. Importantly, for the complex $Cu[TETA]^{2+}$ it was possible to switch between Cu^{2+} in the 100% bound form (pH ≥ 5.01) to 100% free Cu^{2+} (pH ≤ 2.50), *in situ*, simply by generating sufficient protons in the vicinity of the Cu^{2+} detector electrode. This is of interest as it offers the possibility of investigating a wide range of pH dependant equilibrium processes *in-situ*; provided one of the species in the equilibrium is electrochemically active. Moreover, for pH-dependant metal-ligand binding it provides the opportunity to quantify both total and free metal ion concentrations in one measurement, provided the metal can be electrodeposited and subsequently stripped from the surface. This can be performed by simply making a voltammetric measurement of metal concentration at the native solution pH and then by sufficiently lowering the pH to release all the bound metal, making a measurement of total metal concentration. Finally, to achieve low levels of detection (~ ppb) it would be necessary to optimise the generator-detection electrode geometry to provide sufficiently high detection sensitivity, e.g. dual microband electrodes in flow.[19b]

TLR would like to thank the EPSRC and Element Six for funding. JVM thanks the Royal Society for the award of an Industry Fellowship. We all thank Element Six Ltd (Harwell, UK) for provision of the BDD.

Table 1. Comparison of experimentally recorded ASV (i_p / $i_{p,max}$ × 100 %) data as a function of the applied generator current in 100 μM Cu^{2+} and 100 μM TETA solution with 0.1 M KNO_3.

Current Density (mA cm^{-2})	% (i_p /$i_{p,max}$)	Generated pH from Speciation Curve
0.10	0	5.0 ≤
0.20	35	3.8
0.395	79	3.4
1.98	100	≤ 2.5

Notes and references

[a] *Department of Chemistry, University of Warwick, Coventry, CV4 7AL, UK. Fax: +44(0)2476 524112; Tel: +44 (0)2476 573886; E-mail: j.macpherson@warwick.ac.uk*

†Electronic Supplementary Information (ESI) available: S1 Fabrication of the BDD Ring Disc Electrode. S2. Electrochemical Set-Up and Instrumentation. S3 Normalised ASV Data Recorded under In-situ pH Generation Conditions See DOI:

1. (a) Q. Zhang, Z. Hou, B. Louage, D. Zhou, N. Vanparijs, B. G. De Geest and R. Hoogenboom, *Angew. Chem. Int. Edit.*, 2015, **54**, 10879-10883; (b) R. A. Alberty, *J. Biol. Chem.*, 1968, **243**, 1337-1343; (c) S. T. Yang, S. A. White and S. T. Hsu, *Ind. Eng. Chem. Res.*, 1991, **30**, 1335-1342; (d) B. A. Kairdolf and S. Nie, *J. Am. Chem. Soc.*, 2011, **133**, 7268-7271; (e) J. K. Blaho and K. A. Goldsby, *J. Am. Chem. Soc.*, 1990, **112**, 6132-6133; (f) A. Zaban, S. Ferrere, J. Sprague and B. A. Gregg, *J. Phys. Chem. B.*, 1997, **101**, 55-57.
2. C. J. Jones and J. Thornback, *Medicinal Applications of Coordination Chemistry*, Royal Society of Chemistry, 2007.
3. D. R. Williams, *Chem. Rev.*, 1972, **72**, 203-213.
4. F. Fu and Q. Wang, *J. Environ. Manage.*, 2011, **92**, 407-418.
5. K. L. Haas and K. J. Franz, *Chem. Rev.*, 2009, **109**, 4921-4960.
6. *Textbook of Medical Biochemistry*, Elsevier Health Sciences APAC, 2014.
7. T. M. Florence, *Analyst*, 1986, **111**, 489-505.
8. (a) A. Tessier and D. R. Turner, *Metal speciation and bioavailability in aquatic systems*, J. Wiley, 1995; (b) B. Salbu and E. Steinnes, *Trace Elements in Natural Waters*, CRC-Press, 1994.
9. L. M. Mosley, R. Daly, D. Palmer, P. Yeates, C. Dallimore, T. Biswas and S. L. Simpson, *Appl. Geochem.*, 2015, **59**, 1-10.
10. M. Pesavento, *Anal. Chim. Acta*, 1983, **153**, 249-255.
11. G. Hanrahan, *Modelling of Pollutants in Complex Environmental Systems*, ILM Publications, 2010.
12. D. C. Harris, *Quantitative Chemical Analysis*, W. H. Freeman, 2010.
13. (a) E. Hamidi-Asl, D. Daems, K. De Wael, G. Van Camp and L. J. Nagels, *Anal. Chem.*, 2014, **86**, 12243-12249; (b) Y. Y. He, M. Luo, X. Y. Zhang and J. Meng, *Electrochim. Acta*, 2015, **165**, 416-421.
14. J. Sestak, in *Science of heat and thermophysical studies: a generalized approach to thermal analysis*, Elsevier, 2005, ch. 12, pp. 344-377.
15. N. A. Ghalwa, M. Hamada, H. M. Abu-shawish, A. A. Swareh, M. A. Askalany and T. Siam, *J. Electroanal. Chem.*, 2012, **664**, 7-13.
16. G. Aragay, J. Pons and A. Merkoçi, *Chem. Rev.*, 2011, **111**, 3433-3458.
17. (a) W. F. Pickering, in *Chemical Speciation in the Environment*, Blackwell Science Ltd, 2007, DOI: 10.1002/9780470988312.ch2, pp. 7-29; (b) T. Midorikawa, E. Tanoue and Y. Sugimura, *Anal. Chem.*, 1990, **62**, 1737-1746.
18. (a) N. M. Contento and P. W. Bohn, *Biomicrofluidics*, 2014, **8**, 044120; (b) N. M. Contento, S. P. Branagan and P. W. Bohn, *Lab Chip*, 2011, **11**, 3634-3641.
19. (a) T. L. Read, E. Bitziou, M. B. Joseph and J. V. Macpherson, *Anal. Chem.*, 2014, **86**, 367-371; (b) E. Bitziou, M. B. Joseph, T. L. Read, N. Palmer, T. Mollart, M. E. Newton and J. V. Macpherson, *Anal. Chem.*, 2014, **86**, 10834-10840.
20. M. G. Afshar, G. A. Crespo and E. Bakker, *Angew. Chem. Int. Edit.*, 2015, **54**, 8110-8113.
21. L. Rassaei and F. Marken, *Anal. Chem.*, 2010, **82**, 7063-7067.
22. W. Kaim and J. Rall, *Angew. Chem. Int. Edit.*, 1996, **35**, 43-60.
23. R. A. Wuana and F. E. Okieimen, *ISRN Ecol.*, 2011, **2011**, 20.
24. G. J. Brewer, *Clin. Neurophysiol.*, 2010, **121**, 459-460.
25. J. M. Walshe, *Lancet*, 1982, **319**, 643-647.
26. V. M. Nurchi, G. Crisponi, M. Crespo-Alonso, J. I. Lachowicz, Z. Szewczuk and G. J. S. Cooper, *Dalton Trans.*, 2013, **42**, 6161-6170.
27. J. R. Lalanne, F. Carmona, L. Servant and L. Servant, *Optical Spectroscopies of Electronic Absorption*, World Scientific, 1999.
28. H. Angerstein-Kozlowska, B. E. Conway and W. B. A. Sharp, *J. Electroanal. Chem. Interfacial Electrochem.*, 1973, **43**, 9-36.
29. G. E. Batley, *Trace Element Speciation Analytical Methods and Problems*, Taylor & Francis, 1989.
30. F. A. J. Armstrong, *Anal. Chem.*, 1963, **35**, 1292-1294.